Model for temperature anisotropy relaxation in non-neutral plasmas

Louis Jose,[a] Jarett LeVan,[b] and Scott D. Baalrud[c]
Nuclear Engineering & Radiological Sciences, University of Michigan, Ann Arbor, Michigan 48109, USA

(Dated: 20 June 2025)

Non-neutral plasma experiments are excellent benchmarks for validating transport models, including in strongly coupled conditions. Experiments with Penning-Malmberg traps operate under the Brillouin limit, which means that the plasma is also strongly magnetized in the sense that the gyrofrequency exceeds the plasma frequency. This is an unusual regime that is not described by traditional plasma kinetic theory, particularly when strong coupling and strong magnetization are both present. Here, we apply a recently developed generalized Boltzmann kinetic theory to compute the temperature anisotropy relaxation rate in this regime. Strong magnetization is found to severely suppress energy exchange during collisions, leading to a drastically reduced anisotropy relaxation rate. The results exhibit good agreement with previous work by Glinsky et al. when the plasma is weakly coupled, and extends the calculation to the strongly coupled regime as well. Results are compared with published experimental measurements, demonstrating good agreement. Furthermore, the model is tested using molecular dynamics simulations over a broader range of parameters than the experiments reached. These simulations utilize a new Green-Kubo relation, enabling an equilibrium simulation method that is more accurate than previous non-equilibrium methods that have been applied to this problem. Finally, a discussion of detailed balance in strongly magnetized plasmas is provided. Specifically, it is shown that despite the absence of time-reversal symmetry, which is usually used to mathematically prove detailed balance, the results satisfy detailed balance to a high degree of numerical precision.

I. INTRODUCTION

Non-neutral plasmas of pure electrons or pure ions are well diagnosed systems that make excellent benchmark experiments to test models for plasma transport. The most common type of experiment confines the plasma in a Penning-Malmberg trap. The density in a Penning-Malmberg trap is typically below the Brillouin limit.[1] This means that the plasma is strongly magnetized in the sense that the gyrofrequency significantly exceeds the plasma frequency,[2–4] i.e., $\beta = \omega_c/\omega_p > 1$, where $\omega_c = eB/mc$ and $\omega_p = \sqrt{4\pi e^2 n/m}$. Previous theoretical models of non-neutral plasmas primarily considered the weakly coupled, strongly magnetized regime.[5,6] Here, we consider the temperature anisotropy relaxation of a non-neutral plasma as a means to test a generalized kinetic theory that treats a broad range of coupling and magnetization strength regimes.[7] Predictions are compared with previously published experimental measurements,[8,9] and new molecular dynamics (MD) simulations. Here, strong coupling refers to conditions where the potential energy at the average interparticle spacing exceeds the average kinetic energy: $\Gamma = (e^2/a)/(k_B T) > 1$, where $a = [3/(4\pi n)]^{1/3}$ is the Wigner-Seitz radius. Understanding transport in strongly magnetized, strongly coupled plasmas has applications not only in non-neutral plasma experiments,[8–10] but also antimatter trap plasmas,[11–14] magnetized dusty plasmas,[15,16] magnetized ultracold neutral plasmas,[17–22] pinch experiments,[23] electron cooling devices,[24–26] and astrophysical systems such as the atmosphere of neutron stars.[27]

As an example for how testing models in non-neutral plasma experiments can contribute to other research areas, previous works have drawn parallels between the Salpeter enhancement of nuclear reaction rates in stars[28] and the enhancement of temperature anisotropy relaxation due to strong coupling in non-neutral plasmas.[8,10,29] Strong magnetization in a non-neutral plasma causes the perpendicular kinetic energy to act as an adiabatic invariant, significantly inhibiting perpendicular energy exchange during long-range collisions.[6] Energy exchange primarily occurs during short-range collisions where adiabatic invariance is broken, drawing an analogy with the close collisions responsible for fusion reactions. As plasmas become strongly coupled, screening increases the probability of these close collisions, leading to enhanced relaxation rates. Thus, a measurement of the screening effect on the temperature anisotropy relaxation is a proxy for the screening effect in fusion reactions.

Here, we use the same temperature anisotropy relaxation process and experimental measurements to test a new generalized plasma kinetic theory. Considering an initial state with a small temperature anisotropy, the temperature parallel and perpendicular to the magnetic field is expected to relax linearly according to[30,31]

$$\frac{dT_\perp}{dt} = -\frac{1}{2}\frac{dT_\parallel}{dt} = -\nu(T_\perp - T_\parallel), \tag{1}$$

where ν is the anisotropy relaxation rate. Here, a uniform magnetic field is assumed and $\parallel$ and $\perp$ refers to directions parallel and perpendicular to the magnetic field. This process has been modeled using a variety of different theories over the years.[5,6,31,32] Each model is developed based on expansions associated with assumed

[a] Electronic mail: louijos@umich.edu
[b] Electronic mail: jarettl@umich.edu
[c] Electronic mail: baalrud@umich.edu

limits of the coupling and magnetization strength. In order to appreciate the relevant parameter regimes, consider the coupling-magnetization parameter space proposed in Ref. 2 and shown in Fig. 1. This compares the gyroradius ($r_c = \sqrt{k_B T/m}/\omega_c$) with the other length scales relevant to collisions: Coulomb collision mean free path ($\lambda_{\rm col}$), Debye length ($\lambda_D = \sqrt{k_B T/4\pi e^2 n}$), Landau length ($r_L = e^2/k_B T$), and interparticle spacing $a = (3/4\pi n)^{1/3}$.

The unmagnetized regime (1) corresponds to conditions were collisions inhibit the gyromotion of particles and therefore the magnetic field has little influence on transport (the Hall parameter is small). The weakly magnetized regime (2) corresponds to conditions where particles can gyrate, but the gyromotion occurs at a length scale that is much larger than the interaction scale. Therefore the magnetic field does not directly influence the collision operator of the kinetic theory. Regions (1) and (2) are well described by standard plasma kinetic theories, such as the Landau,[33] Rosenbluth,[34] Boltzmann,[35] or Lenard–Balescu[36,37] equations when the plasma is weakly coupled ($\Gamma \ll 1$). Mean force kinetic theory[38,39] is an approach that extends this into the strongly coupled regime ($\Gamma \lesssim 20$). Strong magnetization effects arise in regions (3) and (4), where the gyromotion of particles occurs within the interaction length scale. This is divided into two regions: the strongly magnetized regime (3) where gyromotion occurs between the distance of closest approach and Debye length, and extremely magnetized regime (4) were the gyroradius is smaller than the distance of closest approach (or interparticle spacing for $\Gamma > 1$).

Previous work on strongly magnetized plasmas includes O'Neil's Boltzmann-like kinetic theory,[40] which treats the extremely magnetized regime (4) for weak coupling $\Gamma \ll 1$. Analytic expressions for the temperature anisotropy relaxation rate in this regime were derived by O'Neil and Hjorth,[6] and later modified by Glinsky et al.[5] Numerical results for the case where the gyroradius is comparable to the distance of closest approach (boundary of regime 3 and 4) were also obtained by Glinsky et al.[5] For the intermediate regime (3), previous work has proposed that strong magnetization simply changes the standard plasma kinetic theory by replacing the Debye length with the gyroradius in the Coulomb logarithm.[41–44] Each of these previous models addresses a portion of the strong magnetization parameter space at weak coupling ($\Gamma \ll 1$), but does not address strong coupling. One approach that has been used to attempt to extend the results to strong coupling is to increase the predicted relaxation rate from Glinsky[5] by an enhancement factor derived from a model for an unmagnetized plasma.[8,10,29] This has shown to reproduce experimental measurements of the anisotropy relaxation rate,[8,10] but it is based on an assumption that the strong magnetization and strong coupling effects can be separated and multiplied to obtain the total, rather than deriving a theory self-consistently.

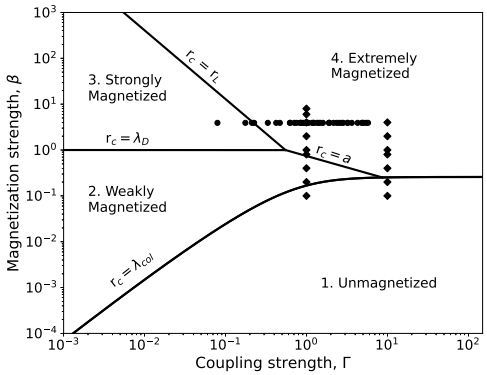

FIG. 1: Magnetization coupling parameter space showing four regimes where transport is influenced by different fundamental processes. Diamonds indicate the conditions where MD simulation data was obtained and circles indicate the conditions where previous experimental data was obtained (Ref. 8). The generalized kinetic theory is expected to apply to any region of this parameter space with $\Gamma \lesssim 20$.

Here, we apply the recent generalized kinetic equation, which attempts to account for strong magnetization and strong coupling self-consistently.[45] This is expected to apply throughout the coupling-magnetization parameter space shown in Fig. 1, with the caveat that the coupling strength is below the liquid like regime ($\Gamma \lesssim 20$). The theory generalizes the traditional Boltzmann kinetic equation to account for the Lorentz force acting on particles during Coulomb collisions. It models strong correlation effects by incorporating the mean force kinetic theory construct[38,39] by modeling the binary interactions using the potential of mean force. The generalized kinetic theory has previously been tested by comparing its predictions for the friction force on a test charge moving through a strongly magnetized plasma with results from MD simulations.[45,46]

Considering temperature anisotropy relaxation, we find that the generalized kinetic theory reproduces Glinsky's results in the weakly coupled, extremely magnetized limit (4) and recovers the standard plasma theory results when the plasma is weakly magnetized (regions 1 and 2). Furthermore, we use the theory to investigate the strongly magnetized regime (3). In this regime, our results do not agree with the previously suggested simple modifications to the Coulomb logarithm[41–44] (for the coupling strengths considered $\Gamma = 0.01$ to 10). Finally, we extend the theory to strongly magnetized strongly coupled plasmas, a regime where previous theoretical treatments are not applicable. Here we find that the relaxation rate is enhanced compared to predictions from the models that assume weak correlations.

The model predictions are tested against molecular dynamics (MD) simulations. Here, a novel method is developed to obtain the relaxation rates from equilibrium MD simulations. Previous simulations relied on non-equilibrium methods where an initial temperature anisotropy is imposed and the relaxation observed.[2,31] Though viable, the accuracy of this approach was found to suffer from an anomalous partial relaxation at early times. Here, we avoid this challenge by developing a new Green-Kubo relation[47,48] that enables one to obtain the temperature anisotropy relaxation rate from equilibrium MD simulations.

Results of the model are also compared with previously published experimental data.[8] In strongly magnetized, weakly coupled electron systems, the results show good agreement with experimentally measured relaxation rates.[9] These experiments were previously used to validate the Glinsky theory.[5] Furthermore, the theory is compared with recent experiments that extend the data to strongly coupled conditions,[8] where the Glinsky theory does not apply. We find that the new approach accurately predicts the experimentally observed anisotropy relaxation rates in this regime as well, achieving the goal of self-consistently including the Salpeter enhancement.

Finally, we note that the derivation of transport properties from kinetic equations commonly relies on the principle of detailed balance,[49–51] which posits that each elementary process is balanced by its reverse process at equilibrium. In Boltzmann kinetic theory, this involves identifying an inverse collision corresponding to a given forward collision. In weakly magnetized plasmas, this is achieved by exploiting the invariance of the equations of motion under time-reversal and space-inversion symmetries.[49,51] However, binary collisions in strongly magnetized plasmas lack time-reversal symmetry when the magnetic field is generated externally, making the traditional proof of detailed balance inapplicable. In this work, we examine detailed balance by comparing temperature relaxation rates calculated with and without invoking the assumption. The results are found to be in excellent agreement, validating the assumption's applicability in strongly magnetized plasmas, despite the lack of time or space-inversion symmetries.

The outline of the paper is as follows: Section II details the molecular dynamics implementation for calculating the temperature anisotropy relaxation rate. Section III outlines the derivation of relaxation rates using the generalized Boltzmann kinetic theory. Section IV presents a comparison of the theoretical results with the molecular dynamics simulations, existing theories, and experimental data. Section V obtains the relaxation rates without invoking the detailed balance assumption and compares these results with those obtained using the assumption.

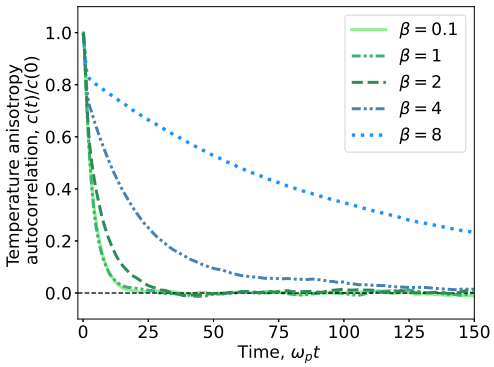

FIG. 2: Temperature anisotropy autocorrelation function for various magnetization strengths [Eq. (6)] computed from MD simulations. Here, the coupling strength is $\Gamma = 1$.

II. MOLECULAR DYNAMICS SIMULATIONS

A. Green-Kubo relation

Previous studies using MD to compute the temperature anisotropy relation rate employed a nonequilibrium method, in which an initial anisotropy was imposed and the temperatures were observed to relax.[2,31] Although this is a viable method, two challenges were encountered. First, an unphysical short-time partial relaxation is observed in strongly magnetized conditions.[31] This is thought to be anomalous and may be associated with an exchange of kinetic and potential energy introduced by the imposition of the temperature anisotropy. Second, non-equilibrium approaches require fitting the time-dependent temperatures to an exponential, even though the decay is not exponential at strong coupling.[31] Here, we avoid these issues by utilizing an equilibrium approach where the relaxation rate is obtained from an integral of a correlation function, similar to the well-established Green-Kubo relations.[47,48] The derivation of this method follows closely to the derivation of the Green-Kubo relations by Zwanzig.[52]

To start, consider the temperature evolution equation from Eq. (1). Conservation of energy can be used to write this as an anisotropy evolution equation

$$\frac{d\Delta T}{dt} = -3\nu\Delta T, \tag{2}$$

where $\Delta T = T_\parallel - T_\perp$. The non-Markoffian generalization of this equation is

$$\frac{d\Delta T}{dt} = -3\int_0^t dt'\,\nu(t-t')\Delta T(t') \tag{3}$$

where $\Delta T = T_\parallel - T_\perp$. Note that a non-Markoffian

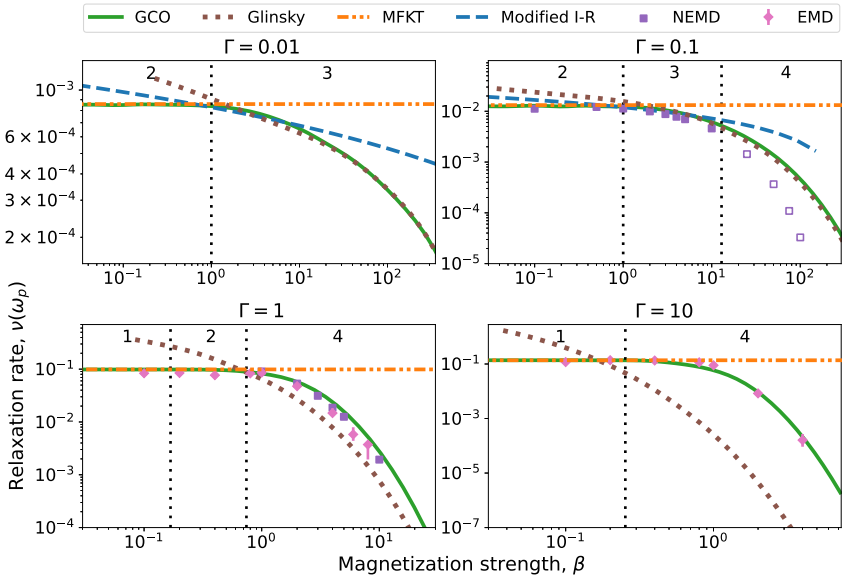

FIG. 3: Temperature anisotropy relaxation rate as a function of magnetization strength for various Coulomb coupling strengths. The green solid lines are the GCO calculations, brown dotted lines are results from Glinksy[5], orange dashed dotted lines are mean force kinetic theory results[38], blue dashed lines are modified Ichimaru-Rosenbluth results[43,44], purple squares are results from Non-equilibrium MD simulations[2] and pink diamonds MD data obtained from equilibrium MD simulations. Hollow squares indicate non-equilibrium MD data points that are not expected to be converged. The numbers on top correspond to the four transport regimes shown in Fig. 1, and vertical dotted lines delineate the boundary.

equation is used here because temperature relaxation in strongly coupled plasmas is non-exponential.[31] The relaxation rate from theory can be interpreted as the zero frequency (long-time) behavior of ν.

A Laplace transform in time of Eq. (3) yields

$$i\omega\Delta\tilde{T}(\omega) - \Delta T(0) = -3\tilde{\nu}(\omega)\Delta\tilde{T}(\omega), \tag{4}$$

where $\tilde{}$ is used to represent a transformed quantity. Multiplying by $\Delta T(0)$ and taking an ensemble average leads to

$$i\omega\tilde{C}(\omega) - C(0) = -3\tilde{\nu}(\omega)\tilde{C}(\omega), \tag{5}$$

where

$$C(t) = \langle \Delta T(t)\Delta T(0)\rangle \tag{6}$$

is the temperature anisotropy autocorrelation function, with $\langle ...\rangle$ representing an ensemble average. Solving Eq. (4) for the frequency-dependent relaxation rate provides

$$\tilde{\nu}(\omega) = \frac{C(0)}{3\tilde{C}(\omega)} - \frac{i\omega}{3}, \tag{7}$$

and an expression for the temperature relaxation rate is obtained by taking the zero frequency limit

$$\nu = \frac{\langle \Delta T(0)\Delta T(0)\rangle}{3\int_0^\infty dt\,\langle \Delta T(t)\Delta T(0)\rangle}. \tag{8}$$

The initial value of the temperature anisotropy autocorrelation function can be determined using the definitions of parallel and perpendicular temperatures from the particle velocities

$$T_\parallel = \frac{2}{Nk_B}\sum_{i=1}^{N}\frac{1}{2}mv_{i,\parallel}^2 \quad \text{and} \quad T_\perp = \frac{1}{Nk_B}\sum_{i=1}^{N}\frac{1}{2}mv_{i,\perp}^2 \tag{9}$$

where $v_{i,\parallel}$ and $v_{i,\perp}$ represent velocities of particle i parallel and perpendicular to the magnetic field. The result is $3T^2/N$, so that Eq. (8) may be written

$$\nu^{-1} = \frac{N}{T^2}\int_0^\infty dt\,\langle \Delta T(t)\Delta T(0)\rangle. \tag{10}$$

Equation (10) is a Green-Kubo relation for the temperature anisotropy relaxation rate that can be evaluated from MD simulations from a time series of particle velocities.

B. Simulation setup

Molecular dynamics simulations were performed using the open-source software LAMMPS.[53] The simulations consisted of 10,000 electrons in a cubic box with periodic boundaries. Each simulation consisted of an equilibration phase of $3000\,\omega_p^{-1}$, followed by a main run. In the equilibration phase, velocities of the particles were thermostat to the desired temperature by applying a Nose-Hoover thermostat.[54] The magnetic field was not included during this phase because the relaxation to equilibrium is faster without it, and the magnetic field is not expected to influence the equilibrium state (the Bohr-van Leeuwen theorem[55,56]). The time step for this phase was chosen as $0.01\,\omega_p^{-1}$. In the main run phase, the thermostat was turned off, and the simulation was run as a microcanonical ensemble. The magnetic field was turned on for this phase, and the time step was chosen as minimum of $0.01\,\omega_p^{-1}$ or $0.01/\beta\,\omega_p^{-1}$ to resolve the gyromotion of the particles.

Parallel and perpendicular temperatures were computed at every timestep from particle velocities from Eq. (9). This data was then used to calculate the temperature anisotropy Green-Kubo relation from Eq. (8). In practice, to evaluate Green-Kubo relations from MD, one must discretize the autocorrelation function in time and impose a cutoff length of L timesteps, where L is chosen such that the autocorrelation has decayed to zero by the time L timesteps have elapsed. Additionally, the ensemble average is generally replaced by a time average, so that one obtains a time-series of length $t_N \gg L$ and averages $t_N - L$ autocorrelation functions together. With these considerations, the relaxation rate was evaluated as

$$\nu = \frac{1}{3\delta t}\frac{\sum_{\tau=0}^{t_N-L}\Delta T(\tau)\Delta T(\tau)}{\sum_{\tau_t=0}^{L}\sum_{\tau=0}^{t_N-L}\Delta T(\tau+\tau_t)\Delta T(\tau)} \tag{11}$$

where τ and τ_t index the timestep (so that ΔT is here considered a function of the timestep number) and δt is the length of a timestep. Figure 2 shows temperature anisotropy autocorrelation obtained using MD simulation for various magnetization strengths. This is integrated to obtain the relaxation rate. Clearly, a stronger magnetic field delays the relaxation and therefore increases the relaxation time, decreasing the relaxation rate.

C. Results

Figure 3 shows the MD simulation results for $\Gamma = 1$ and 10 as a function of magnetization strength. The figure also shows results from previous simulations and theory calculations for $\Gamma = 0.01$ and 0.1. Across all panels, it is evident that regardless of the coupling strength, strong magnetization significantly suppresses the anisotropy relaxation rate, ν, suggesting that temperature anisotropy may persist for extended periods of time in strongly magnetized plasmas. The relaxation rate is unaffected by the magnetization strength in the unmagnetized or magnetized regimes (regions 1 or 2), in agreement with the predictions of standard plasma theories. The relaxation rate gradually decreases in the strongly magnetized regime (region 3), but drops very rapidly with magnetic field strength in the extreme magnetic field regime (region 4). In strongly coupled plasmas, this decrease in relaxation rate with increasing magnetization is steepest. Here, the plasma transitions directly from the unmagnetized to extreme magnetization limits.

Results from the equilibrium method are also compared with previously published results from Ref. 2 that used a nonequilibrium method. For $\Gamma = 1$, both methods are expected to apply, and good agreement is seen in this case. The non-equilibrium method was not applicable to strong coupling because of the unphysical behaviors in the short time scale, and non-exponential relaxation rate, that were described above and in Ref. 2. The new equilibrium method enables one to obtain simulation data in the strongly coupled regime. For $\Gamma = 0.1$, the non-equilibrium results are expected to be trustworthy up to $\beta \approx 10$, but the data beyond this is questionable because finite size effects associated with long-range correlations arise at such high magnetization strengths and weak coupling, which is due to a nearly one-dimensional motion of the particles along field lines.[57] It is expected that these previous results were not converged with respect to the particle number, and are displayed as hollow data points to indicate this. The figure also compares the MD results with predictions of theoretical models, which are described next.

III. THEORY

The temperature evolution can be determined by taking the energy moment of the kinetic equation. We assume an anisotropic Maxwellian velocity distribution function

$$f(\mathbf{v}) = \frac{n}{\pi^{3/2}v_{T\parallel}v_{T\perp}^2}\exp\left(-\frac{v_\perp^2}{v_{T\perp}^2}\right)\exp\left(-\frac{v_\parallel^2}{v_{T\parallel}^2}\right), \tag{12}$$

where $v_{T\parallel} = \sqrt{2k_BT_\parallel/m}$ and $v_{T\perp} = \sqrt{2k_BT_\perp/m}$ are the parallel and perpendicular ion thermal speeds, respectively. This is expected to be an accurate representation of the distribution function for a small temperature anisotropy, and is consistent with the distributions observed in MD simulations. The perpendicular energy moment of the kinetic equation provides

$$\frac{dT_\perp}{dt} = \frac{1}{nk_B}\int d^3\mathbf{v}\frac{mv_\perp^2}{2}\mathcal{C}, \tag{13}$$

where $\mathcal{C}$ is the generalized Boltzmann collision operator (GCO)[7,58]

$$\mathcal{C} = \chi\int d^3\mathbf{v}_2\int_{S_-} ds\,|\mathbf{u}\cdot\hat{\mathbf{s}}|\,\left[f(\mathbf{v}_1')f(\mathbf{v}_2') - f(\mathbf{v}_1)f(\mathbf{v}_2)\right]. \tag{14}$$

Here, $\mathbf{u} = \mathbf{v}_1 - \mathbf{v}_2$ is the relative velocity of the colliding particles, the surface integral is on the surface of the collision volume and $\hat{\mathbf{s}}$ is the unit normal to the $d\mathbf{s}$ surface area. The post collision velocity of each particle ($\mathbf{v}_1'$ and $\mathbf{v}_2'$) are obtained by solving the equations of motion of the colliding particles inside the collision volume

$$m\frac{d\mathbf{V}}{dt} = e\left(\frac{\mathbf{V}}{c}\times\mathbf{B}\right), \tag{15a}$$

$$m\frac{d\mathbf{u}}{dt} = -2\nabla\phi(r) + e\left(\frac{\mathbf{u}}{c}\times\mathbf{B}\right), \tag{15b}$$

where $\mathbf{V} = (\mathbf{v}_1 + \mathbf{v}_2)/2$ is the center of mass velocity. Since the equations of motion for the relative and center of mass velocities separate for a one-component system, only Eq. (15b) needs to be solved to evaluate the collision operator. The interaction between the particles is modeled using the potential of mean force, $\phi(r)$[38,39] which is related to the pair distribution function via $\phi = -k_BT\ln[g(r)]$. Here, the pair distribution function is modeled using the hypernetted-chain approximation for a one-component plasma.[59] For a weakly coupled plasma, the potential of mean force is simply the Debye-Hückel potential.

In addition to obtaining the accurate interaction potential, mean force kinetic theory also considers the Coulomb hole surrounding particles interacting via the Coulomb force. This excluded volume reduces the available space for particles, resulting in an increased collision frequency in strongly coupled plasmas. This phenomenon leads to a frequency enhancement factor, denoted as $\chi[g(r=\sigma)]$, where σ represents the radius of the Coulomb hole, within the collision operator. This factor for plasmas is derived by modifying Enskog's theory of hard spheres.[60] In this model, the χ factor is calculated based on a property of thermodynamic equilibrium, represented by $[g(r)]$, and consequently, it does not depend on the strength of the magnetic field. The values of χ range from 1-1.6, and are provided in Ref. 60.

The GCO from Eq. (14) differs from O'Neil's kinetic equation,[40] which was the basis for Glinsky's previous analysis of temperature anisotropy relaxation,[5] in two respects that enable it to extend to a broader range of magnetization and coupling strength. First, the collision volume described by the 2D surface S_- in Eq. (14) is a sphere with a radius larger than the interaction range. By concentrating on the extreme magnetization regime, O'Neil simplified the collision volume by assuming it has a cylindrical form and that particles only enter or leave the cylinder through the circular end surfaces. This enables a reduced dimensionality to 1D in the surface integral $ds \to 2\pi\rho d\rho$. By keeping a general 2D collision surface, Eq. (14) is able to treat the full range of magnetic field strength, including the usual unmagnetized limit.[7] Second, modeling particle interactions via the mean force, rather than the Coulomb force, in Eq. (15b) brings in aspects of many-body interactions via the appropriate static screening. Previous work has shown that this extends the theory to the strong coupling regime of $\Gamma \lesssim 20$, which is limited only by a transition to a liquid-likes state where other assumptions in the kinetic theory break down.[38,39]

Combining Eqs. (13) and (14), the perpendicular temperature evolution equation is

$$\frac{dT_\perp}{dt} = \frac{\chi}{nk_B}\int d^3\mathbf{v}_1 d^3\mathbf{v}_2 \int_{S_-} d\mathbf{s}\,|\mathbf{u}\cdot\hat{\mathbf{s}}|\frac{1}{2}m\mathbf{v}_{1\perp}^2 [f(\mathbf{v}_1')f(\mathbf{v}_2') - f(\mathbf{v}_1)f(\mathbf{v}_2)]. \tag{16}$$

Section V will discuss evaluating the temperature anisotropy relaxation rate directly from Eq. (16). Here, the expression is further simplified by assuming a principle of detailed balance, as was done in Glinsky[5], with the exception of the different form of the collision operator here. Detailed balance assumes that the collision integral is invariant under interchanging velocities of colliding particles ($\mathbf{v}_1 \leftrightarrow \mathbf{v}_2$ and $\mathbf{v}_1' \leftrightarrow \mathbf{v}_2'$) and interchanging the postcollision velocities with precollision velocities ($\mathbf{v}_1 \leftrightarrow \mathbf{v}_1'$ and $\mathbf{v}_2 \leftrightarrow \mathbf{v}_2'$). Applying these to Eq. (16) provides

$$\frac{dT_\perp}{dt} = \frac{\chi}{nk_B}\int d^3\mathbf{v}_1 d^3\mathbf{v}_2 \int_{S_-} d\mathbf{s}\,|\mathbf{u}\cdot\hat{\mathbf{s}}|\frac{1}{2}m\mathbf{v}_{2\perp}^2 [f(\mathbf{v}_1')f(\mathbf{v}_2') - f(\mathbf{v}_1)f(\mathbf{v}_2)] \tag{17}$$

and

$$\frac{dT_\perp}{dt} = \frac{\chi}{nk_B}\int d^3\mathbf{v}_1' d^3\mathbf{v}_2' \int_{S_-} d\mathbf{s}\,|\mathbf{u}\cdot\hat{\mathbf{s}}|\frac{1}{2}m\mathbf{v}'^2_{1\perp} [f(\mathbf{v}_1)f(\mathbf{v}_2) - f(\mathbf{v}'_1)f(\mathbf{v}'_2)]. \tag{18}$$

Adding Eqs. (16) and (17), then applying Eq. (18) and using the property $d^3\mathbf{v}_1' d^3\mathbf{v}_2' = d^3\mathbf{v}_1 d^3\mathbf{v}_2$ provides

$$\frac{dT_\perp}{dt} = -\frac{\chi}{4nk_B}\int\int d^3\mathbf{v}_1 d^3\mathbf{v}_2 \int_{S_-} d\mathbf{s}\,|\mathbf{u}\cdot\hat{\mathbf{s}}|\Delta E_\perp [f(\mathbf{v}'_1)f(\mathbf{v}'_2) - f(\mathbf{v}_1)f(\mathbf{v}_2)], \tag{19}$$

where

$$\Delta E_\perp = \frac{1}{2}m\left[(\mathbf{v}'^2_{1\perp} + \mathbf{v}'^2_{2\perp}) - (\mathbf{v}^2_{1\perp} + \mathbf{v}^2_{2\perp})\right] \tag{20}$$

is the change in kinetic energy in the perpendicular direction. Rewriting the change in energy in terms of the center of mass and relative frames, and using the fact that the change in energy contribution from the center of mass velocity is zero ($\Delta(\mathbf{V}_\perp^2) = 0$), the change in perpendicular energy can be simplified to

$$\Delta E_\perp = \frac{1}{4}m\Delta(\mathbf{u}_\perp^2), \tag{21}$$

where $\mathbf{u}_\perp = \mathbf{v}_{1\perp} - \mathbf{v}_{2\perp}$, $\mathbf{u}_\perp^2 = \mathbf{u}_\perp\cdot\mathbf{u}_\perp$ and $\Delta(\mathbf{u}_\perp^2) = (\mathbf{u}_\perp^2)' - \mathbf{u}_\perp^2$.

To simplify the temperature evolution equation, the integration variables are transformed from individual particle velocities ($\mathbf{v}_1$, $\mathbf{v}_2$) to center of mass velocity ($\mathbf{V}$) and relative velocity ($\mathbf{u}$). Since the change in perpendicular

energy, $\Delta E_\perp$, and integral on the collision surface are independent of the center of mass velocity, the integration over $\mathbf{V}$ can be performed independently, simplifying the temperature evolution equation to the form

$$\frac{dT_\perp}{dt} = -\frac{nm^{3/2}\chi}{32\pi^{3/2}k_B^{5/2}T_\perp\sqrt{T_\parallel}}\int d^3\mathbf{u}\int_{S_-} d\mathbf{s}\,|\mathbf{u}\cdot\hat{\mathbf{s}}|\Delta E_\perp \exp\left(\frac{-m\mathbf{u}_\parallel^2}{4k_BT_\parallel}\right)\exp\left(\frac{-m\mathbf{u}_\perp^2}{4k_BT_\perp}\right)\left[\exp\left(\frac{-m\mathbf{u}'^2_\parallel + m\mathbf{u}_\parallel^2}{4k_BT_\parallel}\right)\exp\left(\frac{-m\mathbf{u}'^2_\perp + m\mathbf{u}_\perp^2}{4k_BT_\perp}\right) - 1\right] \quad (22)$$

Utilizing energy conservation, $\Delta E_\parallel = -\Delta E_\perp$, and expanding for small temperature anisotropy yields,

$$\frac{dT_\perp}{dt} = \nu(T_\parallel - T_\perp) \quad (23)$$

where

$$\nu = \frac{nm^{3/2}\chi}{32(k_BT)^{7/2}\pi^{3/2}}\int d^3\mathbf{u}\int_{S_-} d\mathbf{s}\,(\Delta E_\perp)^2\,|\mathbf{u}\cdot\hat{\mathbf{s}}| \exp\left(-\frac{m\mathbf{u}^2}{4k_BT}\right) \quad (24)$$

is the temperature anisotropy relaxation rate.

The temperature anisotropy relaxation rate, ν, was obtained by numerically evaluating the 5-D integral in Eq. (24), employing techniques similar to our prior studies.[58,61] Specifically, the integration uses the adaptive Monte Carlo integration code VEGAS.[62,63] For each step of the integration, the change in perpendicular kinetic energy from Eq. (21) was determined by numerically solving the equation of motion from Eq. (15b) using the "DOP 853" method.[64] Several convergence tests were run with respect to number of integration points, and tolerance of the trajectory solver. A typical range of integration points was $10^5 - 10^7$, and the tolerance for trajectory calculations was set within the range of $10^{-8} - 10^{-10}$.

IV. RESULTS AND DISCUSSION

A. Comparison with MD

Figure 3 presents a comparison of the GCO and MD calculations. Excellent agreement is observed in all cases that the MD results are expected to be converged. Notably, the GCO calculations accurately reproduce all trends observed in the MD data, including the suppression of the equilibration rate at high magnetization. The sharp decrease in relaxation rate with increasing coupling strengths at high magnetization observed in MD simulations is also well captured by the GCO. This excellent agreement between the theoretical GCO results and MD simulations, spanning several decades in magnetization-coupling phase space, provides strong verification of the theory.

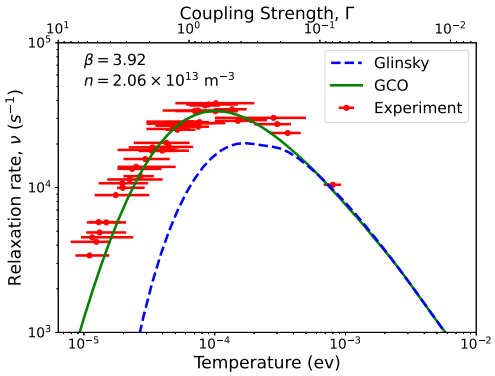

FIG. 4: Comparison of relaxation rate obtained using GCO with an experiment on strongly magnetized magnesium ion in a Penning Malmberg trap[8] and results from Glinksy.[5]

B. Comparison with non-neutral plasma experiments

Figure 4 presents a comparison of the GCO results with measurements conducted on a strongly magnetized magnesium ion plasma in a Penning-Malmberg trap by Anderegg *et al.*[8] These experiments used an applied magnetic field of 1.2 T and an ion density of 2.06×10^{13} m^{-3}, resulting in a magnetization strength of $\beta = 3.92$. The plasma temperature was varied over the range $10^{-5} < T < 10^{-3}$, spanning a coupling range of $0.1 \lesssim \Gamma \lesssim 6$. The figure shows good agreement between the theoretical prediction and experimentally measured relaxation rates. The prediction from Glinsky[5] is also shown for comparison. As expected, this deviates from the measurements at the low temperature end, corresponding to the transition to strong coupling ($\Gamma \gtrsim 0.1$). This is because the Glinsky theory models binary interactions with the Coulomb force, which neglects effects of screening that become important at moderate to strong coupling regimes. By modeling interactions using the potential of mean force, the GCO method is found to naturally extend to this range of strong coupling parameters. This comparison provides the first experimental validation of the GCO theory in a strongly magnetized, strongly coupled plasma.

Figure 5 shows a comparison of predictions from the GCO and Glinsky models with a variety of experimental data[9] that was obtained in weakly coupled, strongly magnetized regimes. Here, the relaxation rate is presented as a function of $\bar{\kappa} = \sqrt{2}r_L/r_c$, which is a dimensionless parameter quantifying magnetization strength that was used in much of the previous work.[5,9] A value of $\bar{\kappa} = 1$ corresponds to the boundary between the strong and extreme magnetization regimes (regions 3 and 4) in Fig. 1, and is related to Γ and β as $\bar{\kappa} = \sqrt{6}\Gamma^{3/2}\beta$. Results in

the figure are shown in terms of a reference value of the relaxation rate

$$\bar{\nu} = 2\sqrt{\frac{\pi}{m}}\frac{ne^4}{(k_B T)^{3/2}} = \omega_p\sqrt{\frac{3}{4\pi}}\Gamma^{3/2}. \tag{25}$$

The experimental data was obtained from Ref. 9, which compiles measurements conducted on pure electron plasmas in the late 1980s and early 1990s by Hyatt et al,[42] and Beck et al.[9,65] The plasma in these experiments was always dilute and hot enough to be in a weakly coupled regime. The ability to quantify the relaxation rate in terms of only $\bar{\nu}$ and $\bar{\kappa}$ is a consequence of being in a weakly coupled regime, which is a basic assumption in the previous models.[5,40] It can be traced to using a Coulomb potential to model the equation of motion in Eq. (15b). Indeed, the figure shows excellent agreement between Glinksy's theory and the experimental measurements, as has been shown previously.[5]

In contrast, the GCO predictions depend independently on Γ and β, and cannot be written simply in terms of $\bar{\nu}$ and $\bar{\kappa}$ in the general case. This is a consequence of the potential of mean force depending on Γ, independent of the value of β, in modeling the equation of motion in Eq. (15b). The GCO data for coupling strengths $\Gamma = 0.01$ and 0.1 agree well with the experiments and Glinsky curve at sufficiently large values of $\bar{\kappa}$, but deviate at smaller values. This is simply associated with the finite value of Γ assumed in each of the GCO calculations. It points out the feature that at a finite value of Gamma, the collision rate cannot be captured solely by the kappa parameter. The GCO and Glinsky results converge in the limit of asymptotically small Γ, corresponding to the limit that screening has a negligible affect on the trajectories computed in Eq. (15b). The experimental data shown here corresponds to this asymptotically small Γ regime throughout the range of $\bar{\kappa}$ values shown in the figure.

C. Comparison with previous theoretical predictions

Next, the GCO predictions are compared with previous reduced models that concentrated on either extreme, or weak, magnetization regimes. For extremely magnetized plasmas, where the gyroradius is significantly smaller than the distance of closest approach ($\bar{\kappa} \gg 1$), O'Neil and Hjorth derived analytic expressions for the relaxation rates.[6] These were later extended by Glinsky et al.[5] to also account for weaker field regimes ($\bar{\kappa} \sim 1$) by numerically solving O'Neil's collision operator.[40] Glinsky's results can be written as

$$\nu_G/\bar{\nu} = \frac{2\sqrt{2}}{\sqrt{\pi}} I(\bar{\kappa}), \tag{26}$$

where $I(\bar{\kappa})$ is the result of a numerically tabulated integral. The curves labeled "Glinsky" in Figs. 3, 4 and 5 were obtained by interpolating the data provided in

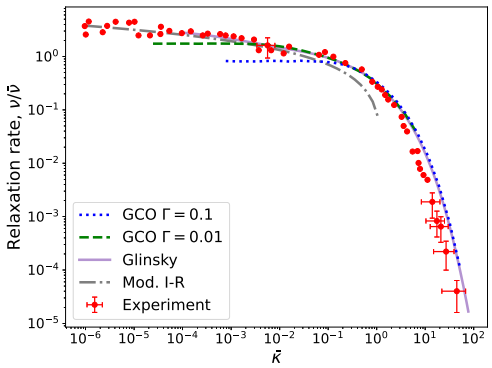

FIG. 5: Comparison of the relaxation rate obtained using GCO with experimental values from Ref. 9 and results from Glinksy[5] and modified Ichimaru-Rosenbluth.[43,44]

Ref. 5 for $I(\bar{\kappa})$. In Fig. 3 the GCO results exhibit good agreement with the Glinsky results for weakly coupled plasmas at high magnetization strengths (regions 3 and 4 for $\Gamma = 0.01$ and 0.1). This trend is also observed in Figs. 4 and 5. As previously mentioned, this agreement is anticipated as the GCO reduces to O'Neil's collision operator in the weakly coupled, extremely magnetized limit. However, the predictions of each model diverge at lower magnetization strengths, because the underlying assumption of a cylindrical collision volume in O'Neil's collision operator is only appropriate in strongly magnetized plasma.

Figures 3 and 4 shows that when plasma becomes strongly coupled, the Glinksy model deviates significantly from GCO. This arises from screening effects via the potential of mean force in Eq. (15b) depending on Γ, a feature absent in Glinsky's theory, which assumes bare Coulomb interactions. Previous works have modeled the strong coupling contributions by multiplying the Glinksy curve by an enhancement factor obtained from a model for the collision frequency in an unmagnetized plasma.[8,10] This leads to a total relaxation rate that is a product of a strong magnetic field effect, and coupling enhancement factor (or Salpeter enhancement factor): $\nu/\bar{\nu} \propto I(\bar{\kappa})f(\Gamma)$.[29] In contrast, GCO obtains relaxation rates by accounting for both the strong coupling effects and strong magnetization simultaneously. The effects are not separable in this formulation.

As discussed in Sec. IV B, Fig. 5 illustrates that the normalized relaxation rate ($\nu/\bar{\nu}$) in Glinsky's model is governed by a single dimensionless parameter ($\bar{\kappa}$), whereas the GCO requires two parameters (Γ and β). The dependence on two-parameters in the GCO is because of using the potential of mean force as the interaction potential in Eq. (15b). This can be simply illustrated

by considering the limit of the Debye-Hückel potential ($\phi(r) = e^2 e^{-r/\lambda_D}/r$), which represents the potential of mean force in the weak coupling limit. In dimensionless units, the relaxation rate Eq. (34) and the equations of motion Eq. (15b) can be written as

$$\frac{\nu}{\bar{\nu}} = \frac{\chi}{64\pi^2} \int d^3\tilde{\mathbf{u}} \int d\tilde{\mathbf{s}} |\tilde{\mathbf{u}} \cdot \hat{\mathbf{s}}| (\Delta\tilde{\mathbf{u}}_\perp^2)^2 e^{-\tilde{\mathbf{u}}^2/2} \quad (27)$$

and

$$\frac{d\tilde{\mathbf{u}}}{d\tilde{t}} = \frac{\exp(-\tilde{r}\frac{r_L}{\lambda_D})}{\tilde{r}^2} \left(1 + \tilde{r}\frac{r_L}{\lambda_D}\right) \hat{\mathbf{r}} + \frac{\bar{\kappa}}{2} \left(\tilde{\mathbf{u}} \times \hat{\mathbf{b}}\right) \quad (28)$$

Here, $\tilde{r} = r/r_L$, and $\tilde{\mathbf{u}} = \mathbf{u}/v_T$. The ratio r_L/λ_D is related to coupling strength by $r_L/\lambda_D = \sqrt{3}\Gamma^{3/2}$. From the equations of motion, Eq. (28), it is clear that the system is characterized by only one parameter ($\bar{\kappa}$) if and only if $r_L/\lambda_D = \sqrt{3}\Gamma^{3/2} \to 0$, which corresponds to the interaction being modeled by the bare Coulomb potential. It is noteworthy that the behavior of weakly coupled, strongly magnetized plasmas can be adequately characterized by a single parameter in Glinsky's model. This is in contrast to weakly magnetized plasmas, where the kinetic theory logarithmically diverges if screening is neglected (the Coulomb logarithm).[30,35,39] This simplification, neglecting the physics of static screening, highlights that a strong magnetic field effectively acts to limit the range of Coulomb interactions.

In the weakly magnetized limit, the GCO results align with the mean force kinetic theory results.[38,39] This is expected since previous works have shown that at weak magnetization, the two are equivalent.[7] Mean force kinetic theory extends the traditional Boltzmann theory to stronger coupling by incorporating the potential of mean force. The temperature anisotropy relaxation rate computed from this is[31]

$$\frac{\nu}{\bar{\nu}} = \frac{2\chi}{15} \Xi^{(2,2)} \quad (29)$$

where the generalized Coulomb logarithm

$$\Xi^{(l,k)} = \frac{1}{2} \int d\xi \xi^{2k+3} e^{-\xi^2} \sigma^{(l)}/\sigma_0 \quad (30)$$

extends the traditional Coulomb logarithm into the strongly coupled regime ($\Gamma \lesssim 20$).[38,66] Here, $\sigma_0 \equiv \pi e^4/(2k_B T)^2$ is a reference cross section, $\xi^2 \equiv u^2/(2v_T^2)$, and $\sigma^{(l)}$ is the l^{th} momentum scattering cross section obtained using the potential of mean force [Eq. (10) in Ref. 66]. In weakly coupled plasmas $\Xi^{(2,2)} = 2\ln\Lambda$, where $\Lambda = \lambda_D/r_L$.

Equation (29) with $\Xi^{(2,2)} = 2\ln\Lambda$ is the same relaxation rate obtained by Ichimaru and Rosenbluth for singly-ionized ions in a magnetized, neutral plasma.[32] This expression is commonly adapted to the strong magnetization regime by replacing the Debye length with the gyroradius in the logarithmic term, i.e., $\Lambda \to \Lambda_m = r_c/r_L$.[9,41,42] This substitution is based on early work by Montgomery[43] and Silin[44], extending plasma kinetic theory to strong magnetization. With this, the "modified Ichimaru-Rosenbluth" relaxation rate is

$$\frac{\nu_{\text{IR}}^m}{\bar{\nu}} = \frac{4}{15} \ln\Lambda_m. \quad (31)$$

The theory is not applicable for extremely magnetized regime, because in this regime $r_c < r_L$, making $\ln\Lambda_m < 0$, leading to a negative relaxation rate. Thus its applicability limited to the strongly magnetized regime (region 3 in Fig. 1). Figure 3 shows that the modified Ichimaru-Rosenbluth (ν_{IR}^m) clearly departs from the other models as β increases. This suggests that the magnetic field's influence is captured differently by this theory compared to others, and a simple substitution of the Debye length with the gyro radius, while economical, may not be accurate, at least for the coupling strengths considered ($\Gamma = 0.01 - 10$). However, Fig. 5 shows that for low values of $\bar{\kappa}$, the modified Ichimaru-Rosenbluth seems to predict the trend in the data well. These low values of $\bar{\kappa}$ correspond to sufficiently small Γ values. Therefore, this method might be more appropriate under much weaker coupling conditions than considered in this work, such as the transition from region 2 to 3 in Fig. 1.

The GCO theory broadly applies across all magnetization strengths within the coupling-magnetization phase space (as depicted in Fig. 1) for $\Gamma \lesssim 20$. While GCO offers a comprehensive approach, it is computationally more demanding than other theories limited to particular regimes. Thus, a breakdown of which theory applies where is useful for efficient and accurate prediction.

For unmagnetized and weakly magnetized plasmas (regimes (1) and (2)), when the plasma is weakly coupled ($\Gamma \ll 1$), standard plasma kinetic theories such as Landau, Rosenbluth, Boltzmann, or Lenard-Balescu are suitable. Conversely, when these plasmas are strongly coupled ($\Gamma \gtrsim 0.1$), mean force kinetic theory provides better results. In weakly coupled, strongly magnetized regimes ($\beta > 1$), Glinksy's tabulated results offer the most accurate approach. The modified Ichimaru-Rosenbluth theory is restricted to very weak coupling ($\Gamma \ll 0.01$) and only applicable at the boundary between regions 2 and 3 ($\beta \approx 1$). Finally, for strongly coupled and strongly magnetized plasmas ($\Gamma > 0.1$ and $\beta \geq 1$), GCO theory stands out as the sole viable candidate.

V. DISCUSSION ON DETAILED BALANCE

In deriving transport coefficients from the kinetic equation, it is common to rely on the principle of detailed balance to simplify the collisional integral. In Sec. III, we used the principle of detailed balance to obtain Eq. (19) from Eq. (16). The principle of detailed balance [Eqs. (17) and (18)] relies on finding an inverse collision for each forward collision. The inverse collision is obtained by interchanging the precollision and postcollision states. Specifically, in a forward collision, particles

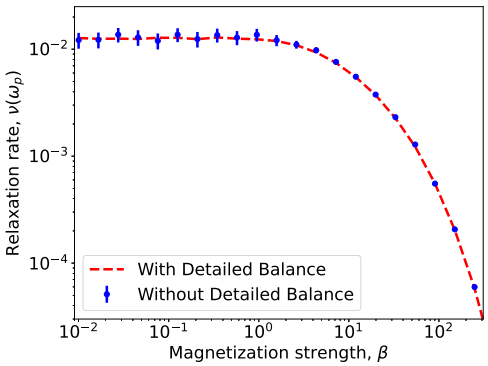

FIG. 6: Results of the temperature anisotropy relaxation rate obtained with the detailed balance [Eq. (24)] (red dashed line) and without [Eq. (34)] (blue dots). Here, the coupling strength is $\Gamma = 0.1$.

enter the collision volume with velocities $\mathbf{v}_1$ and $\mathbf{v}_2$ and exit with velocities $\mathbf{v}_1'$ and $\mathbf{v}_2'$. Conversely, in an inverse collision, particles enter with $\mathbf{v}_1'$ and $\mathbf{v}_2'$ and exit with $\mathbf{v}_1$ and $\mathbf{v}_2$.

In an unmagnetized plasma, the inverse collision is obtained by time reversal followed by spatial inversion. Time reversal maps postcollision velocities to precollision velocities with a sign change ($-\mathbf{v}_1'$, $-\mathbf{v}_2' \to -\mathbf{v}_1$, $-\mathbf{v}_2$), and spatial inversion flips the velocity signs, resulting in ($\mathbf{v}_1'$, $\mathbf{v}_2' \to \mathbf{v}_1$, $\mathbf{v}_2$). These operations are valid due to the invariance of the equations of motion under time reversal and spatial inversion. However, in magnetized plasmas, the Lorentz force during Coulomb collisions breaks time-reversal symmetry, invalidating the invariance of the equations of motion under time reversal. Complete time reversal symmetry is only captured if the currents generating the magnetic field are also included in the system,[67] but here the magnetic field is assumed to be supplied externally. Consequently, the above procedure for obtaining inverse collisions fails. To rigorously assess the applicability of detailed balance in such scenarios, we calculate the anisotropy relaxation rate without invoking this assumption and compare the result with what was obtained with the assumption.

Returning to Eq. (16), before the detailed balance assumption was used, velocity variables are transformed to center-of-mass and relative coordinates, followed by integration over the center-of-mass velocity to obtain

$$\frac{dT_\perp}{dt} = \frac{\chi n}{4\sqrt{2}}\left(\frac{m}{2\pi T_\parallel}\right)^{\frac{1}{2}}\left(\frac{m}{2\pi T_\perp}\right)\int d^3\mathbf{u}\int_{S_-} d\mathbf{s}\,|\mathbf{u}\cdot\hat{\mathbf{s}}| \left(T_\perp + \frac{m\mathbf{u}_\perp{}^2}{4}\right)\exp\left(\frac{-m\mathbf{u}_\parallel^2}{4T_\parallel}\right)\exp\left(\frac{-m\mathbf{u}_\perp^2}{4T_\perp}\right) \left[\exp\left(\frac{-m\mathbf{u}'^2_\parallel + m\mathbf{u}_\parallel^2}{4T_\parallel}\right)\exp\left(\frac{-m\mathbf{u}'^2_\perp + m\mathbf{u}_\perp^2}{4T_\perp}\right) - 1\right]. \quad (32)$$

Utilizing energy conservation, $\Delta E_\parallel = -\Delta E_\perp$, and expanding for small temperature anisotropy yields,

$$\frac{dT_\perp}{dt} = \nu(T_\parallel - T_\perp) \quad (33)$$

where,

$$\nu = -\frac{\chi n}{T^2 4\sqrt{2}}\left(\frac{m}{2\pi T}\right)^{\frac{3}{2}}\int d^3\mathbf{u}\int_{S_-} d\mathbf{s}|\mathbf{u}\cdot\hat{\mathbf{s}}|\Delta E_\perp \left(T + \frac{m\mathbf{u}_\perp{}^2}{4}\right)\exp\left(\frac{-m\mathbf{u}^2}{4T}\right). \quad (34)$$

Equation (34) was evaluated numerically using a similar approach to the detailed balance case, but the computation presents some additional challenges. Specifically, the integrand in this case exhibits both positive and negative values, corresponding to increases and decreases in perpendicular energy, respectively. This contrasts with the detailed balance case, where the integrand is always positive (due to the squared change in perpendicular energy). Accurately resolving both positive and negative peaks in the five-dimensional integration space is computationally demanding. Consequently, more precise trajectory evaluations and a larger number of integration points was required to ensure accurate calculation of relaxation rates.

Figure 6 shows results of the calculations with and without the detailed balance assumption [Eqs. (24) and (34)]. Results from each calculation are indistinguishable. Here, the coupling strength was chosen to be $\Gamma = 0.1$. A reason detailed balance works here in absence of time reversal symmetry might be that many collisions can lumped together to produce a result with the same consequence as an inverse collision, instead of a single collision. Such an explanation is what is used to justify detailed balance in polyatomic gases where there is no space inversion symmetry.[51] Even though the detailed balance is not proven for the magnetized collisions, these results verify the validity of the assumption for these conditions. A better rigorous mathematical proof is desired.

VI. CONCLUSION

In this work, we used the recently developed generalized Boltzmann kinetic theory to calculate the temperature anisotropy relaxation rate in strongly magnetized plasmas. Irrespective of the coupling strength,

we observed that strong magnetization significantly suppresses the anisotropy relaxation rate, but this is most pronounced in strongly coupled plasmas. At high magnetization strengths, the perpendicular energy of particles becomes an adiabatic invariant, substantially reducing energy exchange between parallel and perpendicular directions during collisions.

The calculated relaxation rates were compared with existing theories, molecular dynamics simulations, and experimental data. In the weakly coupled, strongly magnetized limit, our results agree with those of previous results from Glinsky et al.[5] The new method extends the theory to the strongly coupled regime, showing excellent agreement with molecular dynamics simulations and experimental measurements. We introduced a novel method to extract anisotropy relaxation rates from molecular dynamics simulations based on a Green-Kubo relation, with enables a calculation based on equilibrium MD instead of non-equilibrium methods that can introduce nonphysical effects. Furthermore, we examined the validity of the detailed balance assumption in strongly magnetized plasmas, where time-reversal symmetry is broken. We found that relaxation rates calculated without the detailed balance assumption were in excellent agreement with those calculated using it, validating the assumption's applicability in strongly magnetized plasmas.

In a weakly magnetized ion-electron system, the fastest process is the anisotropy relaxation of the electrons due to electron-electron collisions, which is faster than the ion-electron equilibration time by a factor proportional to the ion-to-electron mass ratio. However, when the electrons become strongly magnetized, the temperature anisotropy relaxation due to electron-electron collisions slows down and becomes considerably slower than the ion-electron relaxation time. Recent work[68] has shown that this leads to novel pathways for temperature relaxation in ion-electron systems. Specifically, the ion temperature equilibrates with the electron parallel temperature, while the perpendicular electron temperature equilibrates with the other temperatures at a much slower rate, determined by the electron-electron anisotropy relaxation rate. These results have significant implications in determining the collisional cooling time of antiprotons with electrons in antimatter traps at the Antihydrogen Laser Physics Apparatus (ALPHA).[13,14]

VII. DATA AVAILABILITY STATEMENT

The data that support the findings of this study are available from the corresponding author upon reasonable request.

VIII. AUTHOR DECLARATIONS

A. Conflict of Interest

The authors have no conflicts to disclose.

ACKNOWLEDGMENTS

The authors thank James C. Welch for helpful conversations during the preparation of the manuscript. This material is based upon work supported by the NSF grant award No. PHY-2205506. It used Expanse at San Diego Supercomputer Center[69] through allocation PHY-150018 from the Advanced Cyberinfrastructure Coordination Ecosystem: Services & Support (ACCESS) program, which is supported by National Science Foundation grants #2138259, #2138286, #2138307, #2137603, and #2138296.

[1] J. R. Danielson, D. H. E. Dubin, R. G. Greaves, and C. M. Surko, "Plasma and trap-based techniques for science with positrons," Rev. Mod. Phys. **87**, 247–306 (2015).
[2] S. D. Baalrud and J. Daligault, "Transport regimes spanning magnetization-coupling phase space," Phys. Rev. E **96**, 043202 (2017).
[3] T. Ott and M. Bonitz, "Diffusion in a strongly coupled magnetized plasma," Physical review letters **107**, 135003 (2011).
[4] T. Ott, M. Bonitz, P. Hartmann, and Z. Donkó, "Spontaneous generation of temperature anisotropy in a strongly coupled magnetized plasma," Phys. Rev. E **95**, 013209 (2017).
[5] M. E. Glinsky, T. M. O'Neil, M. N. Rosenbluth, K. Tsuruta, and S. Ichimaru, "Collisional equipartition rate for a magnetized pure electron plasma," Physics of Fluids B: Plasma Physics **4**, 1156–1166 (1992).
[6] T. O'Neil and P. Hjorth, "Collisional dynamics of a strongly magnetized pure electron plasma," Physics of fluids **28**, 3241–3252 (1985).
[7] L. Jose and S. D. Baalrud, "A generalized boltzmann kinetic theory for strongly magnetized plasmas with application to friction," Physics of Plasmas **27**, 112101 (2020).
[8] F. Anderegg, D. H. E. Dubin, M. Affolter, and C. F. Driscoll, "Measurements of correlations enhanced collision rates in the mildly correlated regime ($\gamma \sim 1$)," Physics of Plasmas **24**, 092118 (2017), https://pubs.aip.org/aip/pop/article-pdf/doi/10.1063/1.4999350/19771454/092118_1_online.pdf.
[9] B. R. Beck, J. Fajans, and J. H. Malmberg, "Temperature and anisotropic-temperature relaxation measurements in cold, pure-electron plasmas," Physics of Plasmas **3**, 1250–1258 (1996), https://pubs.aip.org/aip/pop/article-pdf/3/4/1250/19084692/1250_1_online.pdf.
[10] F. Anderegg, D. H. E. Dubin, T. M. O'Neil, and C. F. Driscoll, "Measurement of correlation-enhanced collision rates," Phys. Rev. Lett. **102**, 185001 (2009).
[11] J. Fajans and C. Surko, "Plasma and trap-based techniques for science with antimatter," Physics of Plasmas **27**, 030601 (2020).
[12] E. V. Stenson, J. Horn-Stanja, M. R. Stoneking, and T. S. Pedersen, "Debye length and plasma skin depth: two length scales of interest in the creation and diagnosis of laboratory pair plasmas," Journal of Plasma Physics **83**, 595830106 (2017).
[13] M. Ahmadi, B. X. R. Alves, C. J. Baker, W. Bertsche, E. Butler, A. Capra, C. Carruth, C. L. Cesar, M. Charlton, S. Cohen, R. Collister, S. Eriksson, A. Evans, N. Evetts, J. Fajans, T. Friesen, M. C. Fujiwara, D. R. Gill, A. Gutierrez, J. S. Hangst, W. N. Hardy, M. E. Hayden, C. A. Isaac, A. Ishida,

M. A. Johnson, S. A. Jones, S. Jonsell, L. Kurchaninov, N. Madsen, M. Mathers, D. Maxwell, J. T. K. McKenna, S. Menary, J. M. Michan, T. Momose, J. J. Munich, P. Nolan, K. Olchanski, A. Olin, P. Pusa, C. Ø. Rasmussen, F. Robicheaux, R. L. Sacramento, M. Sameed, E. Sarid, D. M. Silveira, S. Stracka, G. Stutter, C. So, T. D. Tharp, J. E. Thompson, R. I. Thompson, D. P. van der Werf, and J. S. Wurtele, "Antihydrogen accumulation for fundamental symmetry tests," Nature Communications **8**, 681 (2017).

[14]C. J. Baker, W. Bertsche, A. Capra, C. L. Cesar, M. Charlton, A. C. Mathad, S. Eriksson, A. Evans, N. Evetts, S. Fabbri, J. Fajans, T. Friesen, M. C. Fujiwara, P. Grandemange, P. Granum, J. S. Hangst, M. E. Hayden, D. Hodgkinson, C. A. Isaac, M. A. Johnson, J. M. Jones, S. A. Jones, S. Jonsell, L. Kurchaninov, N. Madsen, D. Maxwell, J. T. K. McKenna, S. Menary, T. Momose, P. Mullan, K. Olchanski, A. Olin, J. Peszka, A. Powell, P. Pusa, C. Ø. Rasmussen, F. Robicheaux, R. L. Sacramento, M. Sameed, E. Sarid, D. M. Silveira, G. Stutter, C. So, T. D. Tharp, R. I. Thompson, D. P. van der Werf, and J. S. Wurtele, "Sympathetic cooling of positrons to cryogenic temperatures for antihydrogen production," Nature Communications **12**, 6139 (2021).

[15]E. Thomas, R. L. Merlino, and M. Rosenberg, "Magnetized dusty plasmas: the next frontier for complex plasma research," Plasma Physics and Controlled Fusion **54**, 124034 (2012).

[16]M. Menati, S. Williams, B. Rasoolian, E. Thomas, and U. Konopka, "Formation of turing patterns in strongly magnetized electric discharges," Communications Physics **6**, 221 (2023).

[17]G. M. Gorman, M. K. Warrens, S. J. Bradshaw, and T. C. Killian, "Laser-induced-fluorescence imaging of a spin-polarized ultracold neutral plasma in a magnetic field," Phys. Rev. A **105**, 013108 (2022).

[18]G. M. Gorman, M. K. Warrens, S. J. Bradshaw, and T. C. Killian, "Magnetic confinement of an ultracold neutral plasma," Phys. Rev. Lett. **126**, 085002 (2021).

[19]X. L. Zhang, R. S. Fletcher, S. L. Rolston, P. N. Guzdar, and M. Swisdak, "Ultracold plasma expansion in a magnetic field," Phys. Rev. Lett. **100**, 235002 (2008).

[20]R. T. Sprenkle, S. D. Bergeson, L. G. Silvestri, and M. S. Murillo, "Ultracold neutral plasma expansion in a strong uniform magnetic field," Phys. Rev. E **105**, 045201 (2022).

[21]J. M. Guthrie and J. L. Roberts, "Finite-amplitude rf heating rates for magnetized electrons in neutral plasma," Physics of Plasmas **28**, 052101 (2021), https://doi.org/10.1063/5.0047640.

[22]C. Pak, V. Billings, M. Schlitters, S. D. Bergeson, and M. S. Murillo, "Preliminary study of plasma modes and electron-ion collisions in partially magnetized strongly coupled plasmas," Phys. Rev. E **109**, 015201 (2024).

[23]N. Bennett, D. R. Welch, G. Laity, D. V. Rose, and M. E. Cuneo, "Magnetized particle transport in multi-ma accelerators," Phys. Rev. Accel. Beams **24**, 060401 (2021).

[24]L. I. Men'shikov, "New directions in the theory of electron cooling," Physics-Uspekhi **51**, 645–680 (2008).

[25]Y. S. Derbenev and A. N. Skrinsky, "The Effect of an Accompanying Magnetic Field on Electron Cooling," Part. Accel. **8**, 235–243 (1978).

[26]V. Parkhomchuk, "Study of fast electron cooling," in *Proceedings of the Workshop on Electron Cooling and Related Applications (ECOOL84, 1984)*, edited by H. Poth (Kernforschungszentrum Karlsruhe GmbH, Karlsruhe, 1984) pp. 71–84.

[27]A. K. Harding and D. Lai, "Physics of strongly magnetized neutron stars," Reports on Progress in Physics **69**, 2631 (2006).

[28]E. E. Salpeter and H. M. van Horn, "Nuclear Reaction Rates at High Densities," Astrophys. J. **155**, 183 (1969).

[29]D. H. E. Dubin, "Measurement of screening enhancement to nuclear reaction rates using a strongly magnetized and strongly correlated non-neutral plasma," Phys. Rev. Lett. **94**, 025002 (2005).

[30]S. Ichimaru, *Statistical Plasma Physics, Volume I: Basic Principles* (CRC Press, 2004).

[31]S. D. Baalrud and J. Daligault, "Temperature anisotropy relaxation of the one-component plasma," Contributions to Plasma Physics **57**, 238–251 (2017), https://onlinelibrary.wiley.com/doi/pdf/10.1002/ctpp.201700028.

[32]S. Ichimaru and M. N. Rosenbluth, "Relaxation processes in plasmas with magnetic field. temperature relaxations," The Physics of Fluids **13**, 2778–2789 (1970), https://aip.scitation.org/doi/pdf/10.1063/1.1692864.

[33]L. D. Landau, "The transport equation in the case of coulomb interactions," in *Collected Papers of L.D. Landau*, edited by D. TER HAAR (Pergamon, 1965) pp. 163–170.

[34]M. N. Rosenbluth, W. M. MacDonald, and D. L. Judd, "Fokker-planck equation for an inverse-square force," Phys. Rev. **107**, 1–6 (1957).

[35]J. H. Ferziger and H. G. Kaper, *Mathematical theory of transport processes in gases* (North-Holland, 1972).

[36]A. Lenard, "On bogoliubov's kinetic equation for a spatially homogeneous plasma," Annals of Physics **10**, 390–400 (1960).

[37]R. Balescu, "Irreversible processes in ionized gases," The Physics of Fluids **3**, 52–63 (1960), https://aip.scitation.org/doi/pdf/10.1063/1.1706002.

[38]S. D. Baalrud and J. Daligault, "Effective potential theory for transport coefficients across coupling regimes," Phys. Rev. Lett. **110**, 235001 (2013).

[39]S. D. Baalrud and J. Daligault, "Mean force kinetic theory: A convergent kinetic theory for weakly and strongly coupled plasmas," Physics of Plasmas **26**, 082106 (2019).

[40]T. O'Neil, "Collision operator for a strongly magnetized pure electron plasma," Physics of Fluids **26**, 2128–2135 (1983).

[41]J. Rand McNally, "Simple physical model for the effect of a magnetic field on the coulomb logarithm for test ions slowing down on electrons in a plasma," Nuclear Fusion **15**, 344 (1975).

[42]A. W. Hyatt, C. F. Driscoll, and J. H. Malmberg, "Measurement of the anisotropic temperature relaxation rate in a pure electron plasma," Phys. Rev. Lett. **59**, 2975–2978 (1987).

[43]D. Montgomery, G. Joyce, and L. Turner, "Magnetic field dependence of plasma relaxation times," Physics of Fluids **17**, 2201–2204 (1974).

[44]V. Silin, "On relaxation of electron and ion temperatures of fully ionized plasma in a strong magnetic field," Sov. Phys. JETP **16**, 1281 (1963).

[45]L. Jose and S. D. Baalrud, "A kinetic model of friction in strongly coupled strongly magnetized plasmas," Physics of Plasmas **28**, 072107 (2021), https://doi.org/10.1063/5.0054552.

[46]L. Jose, D. J. Bernstein, and S. D. Baalrud, "Barkas effect in strongly magnetized plasmas," Physics of Plasmas **29**, 112103 (2022), https://doi.org/10.1063/5.0121285.

[47]M. S. Green, "Markoff random processes and the statistical mechanics of time-dependent phenomena. ii. irreversible processes in fluids," The Journal of Chemical Physics **22**, 398–413 (1954).

[48]R. Kubo, M. Yokota, and S. Nakajima, "Statistical-mechanical theory of irreversible processes. ii. response to thermal disturbance," Journal of the Physical Society of Japan **12**, 1203–1211 (1957).

[49]F. Reif, *Fundamentals of statistical and thermal physics* (Waveland Press, 2009).

[50]C. Cercignani, R. Illner, and M. Pulvirenti, *The mathematical theory of dilute gases*, Vol. 106 (Springer-Verlag New York, 1994).

[51]C. Cercignani and M. Lampis, "On the h-theorem for polyatomic gases," Journal of Statistical Physics **26**, 795–801 (1981).

[52]R. Zwanzig, "Elementary derivation of time-correlation formulas for transport coefficients," The Journal of Chemical Physics **40**, 2527–2533 (1964), https://pubs.aip.org/aip/jcp/article-pdf/40/9/2527/18833421/2527_1_online.pdf.

[53]A. P. Thompson, H. M. Aktulga, R. Berger, D. S. Bolintineanu, W. M. Brown, P. S. Crozier, P. J. in 't Veld, A. Kohlmeyer, S. G. Moore, T. D. Nguyen, R. Shan, M. J. Stevens, J. Tranchida, C. Trott, and S. J. Plimpton, "LAMMPS - a flexible simulation tool for particle-based materials modeling at the atomic, meso, and continuum scales," Comp. Phys. Comm. **271**, 108171 (2022).

[54]D. Frenkel and B. Smit, "Chapter 6 - molecular dynamics in various ensembles," in *Understanding Molecular Simulation (Second Edition)* (Academic Press, San Diego, 2002) second edition ed., pp. 139–163.
[55]"Ii. the doctor's dissertation (text and translation)**[see introduction, sect. 2.]," in *EARLY WORK (1905–1911)*, Niels Bohr Collected Works, Vol. 1, edited by L. Rosenfeld and J. R. Nielsen (Elsevier, 1972) pp. 163–393.
[56]Van Leeuwen, H.-J., "Problèmes de la théorie électronique du magnétisme," J. Phys. Radium **2**, 361–377 (1921).
[57]K. R. Vidal and S. D. Baalrud, "Extended space and time correlations in strongly magnetized plasmas," Physics of Plasmas **28**, 042103 (2021).
[58]L. Jose, *Kinetic Theory of Strongly Magnetized Plasmas*, Ph.D. thesis, University of Michigan (2023).
[59]J. P. Hansen and I. R. McDonald, *Theory of simple liquids: with applications to soft matter* (Academic Press, 2013).
[60]S. D. Baalrud and J. Daligault, "Modified enskog kinetic theory for strongly coupled plasmas," Phys. Rev. E **91**, 063107 (2015).
[61]L. Jose and S. D. Baalrud, "Theory of the ion–electron temperature relaxation rate in strongly magnetized plasmas," Physics of Plasmas **30**, 052103 (2023).
[62]G. P. Lepage, "Adaptive multidimensional integration: vegas enhanced," Journal of Computational Physics **439**, 110386 (2021).
[63]P. Lepage, "gplepage/vegas: vegas version 6.1.3," (2024).
[64]E. Hairer, S. P. Norsett, and G. Wanner, "Runge-kutta and extrapolation methods," in *Solving Ordinary Differential Equations I: Nonstiff Problems* (Springer Berlin Heidelberg, 1993) pp. 129–353.
[65]B. R. Beck, J. Fajans, and J. H. Malmberg, "Measurement of collisional anisotropic temperature relaxation in a strongly magnetized pure electron plasma," Phys. Rev. Lett. **68**, 317–320 (1992).
[66]S. D. Baalrud and J. Daligault, "Extending plasma transport theory to strong coupling through the concept of an effective interaction potential," Physics of Plasmas **21**, 055707 (2014).
[67]S. R. de. Groot and P. Mazur, *Non-equilibrium thermodynamics* (North-Holland Pub. Co.; Interscience Publishers, 1962).
[68]L. Jose, J. C. Welch, T. D. Tharp, and S. D. Baalrud, "Temperature relaxation rates in strongly magnetized plasmas," Phys. Rev. E **111**, 035201 (2025).
[69]S. Strande, H. Cai, M. Tatineni, W. Pfeiffer, C. Irving, A. Majumdar, D. Mishin, R. Sinkovits, M. Norman, N. Wolter, T. Cooper, I. Altintas, M. Kandes, I. Perez, M. Shantharam, M. Thomas, S. Sivagnanam, and T. Hutton, "Expanse: Computing without boundaries: Architecture, deployment, and early operations experiences of a supercomputer designed for the rapid evolution in science and engineering," in *Practice and Experience in Advanced Research Computing 2021: Evolution Across All Dimensions*, PEARC '21 (Association for Computing Machinery, New York, NY, USA, 2021).